

According to the model of parallel porous bodies (16,17), the rate of flow of each porous body makes its contribution to the total flow. Since the solid volume is $(1-\epsilon_t)$ for unit volume of porous medium, where ϵ_t is the total porosity, k should be reduced by $(1-\epsilon_t)$ times. Then the total flow Q through the unit area of porous medium is the sum of Q_i ,

$$Q = \sum Q_i = \frac{\pi}{8\eta} \cdot \left[\frac{dp}{dx} \sum N_i^2 r_i^4 - \frac{(1-\epsilon_t)\rho k}{M} \sum N_i^2 \right] \quad (2.3.4)$$

However, Eq.(2.3.4) is applicable only to the model of one-dimension cylindrical pores. In the case of the model of intersecting cylindrical pores, the effective pressure gradient increases because the effective length of pores along the gradient is reduced by the intersecting points and some macro-pores, which are too large to be measured by mercury porosimetry (4,6) and complexly distribute inside the space of the porous material. The more the pores are, the greater the increase of effective pressure gradient is. It can be simply assumed the effective length is reduced by $(1-\epsilon_t)$ times. On the other hand, the number of pores in unit area N_i^2 will be affected by pore bodies each other and by macro-pores. It also can be simply assumed that N_i^2 is proportional to the total porosity ϵ_t , although it is difficult to accurately estimate these influences. Then Eq.(2.3.4) can be modified as the following form,

$$Q = \frac{\pi\beta\epsilon_t}{8\eta} \cdot \left[\frac{dp}{dx} \frac{\sum N_i^2 r_i^4}{(1-\epsilon_t)} - \frac{(1-\epsilon_t)\rho k}{M} \sum N_i^2 \right] \quad (2.3.5)$$

where β is a proportional constant. Eq.(2.3.5) illustrates that for a given fluid, the flow does not occur in the pores smaller than a certain size unless the pressure gradient reaches a very high value. It is implied that under a certain range of pressure gradient the total flow does not linearly increase with the increment of pressure gradient until pressure gradient reaches a point at which the flow occurs in all pore bodies (as shown in Fig.2.3.1). This is consistent with what Gjerv (10) and Mills(11) observed. In Fig.2.3.1, the intercept, $(dp/dx)_0$, of the extended line on the axis of pressure gradient reflects the total resistant force applied by pore wall to the fluid. In other words, an extra pressure gradient is needed to overcome the resistant force. $(dp/dx)_0$ can be defined as the maximum extra pressure gradient.

$$\left(\frac{dp}{dx} \right)_0 = \frac{\rho k (1-\epsilon_t)^2 \sum N_i^2}{M \sum N_i^2 r_i^4} \quad (2.3.6)$$

Eq.(2.3.6) implies that the greater the pore size or the porosity, the smaller the value of $(dp/dx)_0$, and that for a certain porosity, the more the small pores the greater the value of $(dp/dx)_0$. It is shown that the permeability of HCP is strongly dependent on the pore size distribution as well as the total porosity. Eq.(2.3.6) also implies that the smaller the density of fluid, the more easily the flow occurs. It explains the fact that gas is much easier to flow through HCP than water.

3 EXPERIMENTAL VERIFICATION

Since Eq.(2.3.5) has rather different conception from previous permeability theories or equations, to verify this equation, it is better to use the experimental data published by other researchers. Thirteen sets of data were used although there are rather limited literatures containing the detail data of pore structure and permeability. Eleven of them were reported by Mehta and Marumohan (4), and the rest were reported by Goto and Roy (6). The water-cement ratio

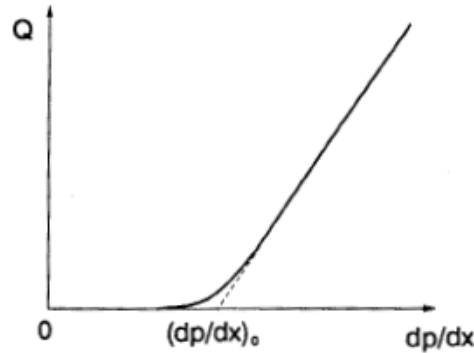


FIG. 2.3.1
Theoretical curve of flow rate versus pressure gradient and maximum extra gradient $(dp/dx)_0$

ranges from 0.3 to 0.9, curing age from 28 days to 1 year and curing temperature from ambient to 60 °C. In order to compare with the data reported by other researchers, the traditional 140° of contact angle of mercury was used to replace 130° assumed by Manmohan and Metha (5). The density of HGP, ρ_s , can be calculated from the bulk density ρ_b and the total porosity ϵ_t ,

$$\rho_s = \rho_b / (1 - \epsilon_t) \quad (3.1)$$

or estimated from the degree of hydration α ,

$$\rho_s = \frac{1 + W_n \alpha}{\frac{(1 + W_n) \alpha}{\rho_g} + \frac{(1 - \alpha)}{\rho_c}} \quad (3.2)$$

where W_n is non-evaporable water, $W_n = 0.25$; ρ_g and ρ_c are the densities of CSH gel and cement, $\rho_g = 2.34 \text{ g/cm}^3$, $\rho_c = 3.15 \text{ g/cm}^3$, respectively. The flow rate can be estimated from the experimental data of permeability coefficient K_l and pressure gradient reported in reference (4). Nine samples (0.5-28 to 0.9-360) containing detail data were used to find the constants β and k on the computer by optimum seeking method. The optimum values were found to be $\beta = 82.1$ and $k = 3.24 \times 10^{-25} \text{ N}\cdot\text{m}^4$. The value of k , as expected just like a general friction, is about 10% as much as the theoretical attractive force. The calculated results are shown in Table 3.1 and the ratios of calculated Q to experimental Q are shown in Fig. 3.1.

It can be seen from Table 3.1 and Fig. 3.1 that the calculated flow rates are well correspondent with the experimental values. The results show that the values of $(dp/dx)_0$ for most of samples are higher than the test pressure gradients (1370 and 187 MPa/m) applied by Mehta (4). It means that most of experimental K_l would change with the gradient. The results imply a reversely proportional relationship between $(dp/dx)_0$ and the experimental K_l . In fact since $K_l \propto Q / (dp/dx)$, whereas $Q \propto \beta \epsilon_t$. It is certain that K_l will be reversely proportional to $(dp/dx)_0 / \beta \epsilon_t$. It is found by further mathematical treatment that the logarithm of K_l has a good correlativity with the logarithm of P_k (as shown in Fig. 3.2), where $P_k = (dp/dx)_0 / \beta \epsilon_t$, can be defined as the intrinsic impermeability coefficient, and

the regressive equation is

$$\log K_1 = 2.994 - 1.091 \log P_k \quad (3.3)$$

The square correlative coefficient R^2 is up to 0.971, greater than that of Eq.(1.1). The calculated K_1 from Eq.(3.1) are also shown in Table 3.1. The ratio of calculated K_1 to experimental K_1 is shown in Fig.3.3.

TABLE 3.1
Calculated Results of Various Samples of HCP

Sample No.	w/c-day-°C	Q_{exp} $\times 10^{-3} \text{m/s}$	Q_{cal} $\times 10^{-3} \text{m/s}$	K_{1exp} $\times 10^{-12} \text{m/s}$	$(dP/dx)_0$ MPa/m	$\sum N_i^2$ $\times 10^{15} \text{m}^{-2}$	$\sum N_i^2 r_i^4$ $\times 10^{15} \text{m}^2$	K_{1cal} $\times 10^{-12} \text{m/s}$
1	0.5-28-a*	0.41	0.41	0.3	39800	0.3195	0.0441	0.48
2	0.6-28-a	3.16	6.85	2.3	6800	0.2848	0.1698	3.9
3	0.7-28-a	4.11	4.11	22.0	1620	0.2801	0.6188	20.1
4	0.8-28-a	18.0	11.6	96.3	574	0.2640	1.4693	65.1
5	0.9-28-a	76.5	49.6	410	99.8	0.2034	4.5272	497
6	0.7-90-a	2.47	2.46	1.8	18500	0.3889	0.0897	1.3
7	0.7-360-a	1.92	1.63	1.4	23200	0.3751	0.0706	1.0
8	0.9-90-a	3.27	4.73	17.5	1530	0.3255	0.5665	24
9	0.9-360-a	1.42	1.41	7.6	6120	0.4888	0.2155	5.2
10	0.3-28-a			0.1	96600	0.1507	0.0147	0.11
11	0.4-28-a			0.2	61600	0.2751	0.0344	0.23
12†	0.4-28-27			0.67	46500	0.4499	0.0448	0.45
13†	0.4-28-60			5.34	3620	0.6288	0.9248	6.74

Note: * a: ambient temperature;

† experimental data reported by Goto and Roy (6), others by Mehta and Manmohan (4).

It is surprising that when directly applying Eq.(3.3) to the data of Samples 0.3-28 and 0.4-28 Metha (4) reported and Samples 0.4-28-27 and 0.4-28-60 Goto (6) reported, the calculated values of K_1 correspond very much with the experimental values (as shown in Table 3.1 and Fig. 3.3), where the total porosity ϵ_t or the bulk density ρ_b was estimated from Eq.(3.1) and (3.2), assuming the hydration degree of Sample 0.4-28-27 as the same as that of Sample 0.4-28, i.e. 0.62, and that of Sample 0.4-28-60 as 0.7.

It can be seen from Fig.3.3 that the values of K_{1cal}/K_{1exp} for thirteen samples fall within the range of 0.68 to 1.72. This accuracy is satisfactory enough.

4 DISCUSSION

As seen from the above result, the value of P_k reflects the impermeability of HCP very well. According to its definition, P_k can be expressed as

$$P_k = \frac{\rho k (1 - \epsilon_t)^2 \sum N_i^2}{\beta M \epsilon_t \sum N_i^2 r_i^4} \quad (4.1)$$

It is apparent that, for a certain fluid, P_k is dominated by pore structure and